

# Design and manufacturing of a soft tourniquet for regulation of arterial occlusion pressure

Juana Camacho<sup>1</sup>, and Jonathan Camargo<sup>2</sup>

**Abstract**—Effective hemorrhage control is critical in emergency medicine, as rapid and efficient intervention can significantly impact patient survival. However, traditional tourniquets that apply static pressure pose risks such as tissue damage, apoptosis, and thrombosis due to excessive compression. To address these risks, this work presents the design and fabrication of a soft robotic tourniquet capable of dynamically adjusting pressure to achieve Arterial Occlusion Pressure (AOP) while reducing tissue damage and clot formation. With soft robotics ring inspired by the longitudinal muscle structures of tardigrades, the proposed design uses internal chambers that contract under negative pressure, applying circumferential compression around the limb. Through simulation-driven design refinement, iterative prototyping, and experimental testing on a venipuncture simulation arm, the tourniquet achieved an internal diameter reduction of 53.95%, demonstrating effective contraction and conformance to the limb. This paper details the research, design process, simulation, and experimental validation of the device, highlighting potential to improve hemorrhage control in medical emergencies. The results contribute to the advancement of wearable medical devices and outline future directions for improving tourniquets through soft robotics technology.

Keywords: soft robotics, design, health and medical applications.

## I. INTRODUCTION

Tourniquets are widely used medical devices for hemorrhage control in both emergency trauma care and surgical procedures. Their primary function is to occlude arterial blood flow in a limb, preventing excessive bleeding and improving survival rates in critical scenarios. However, despite their life-saving role, conventional tourniquets pose significant risks when not properly calibrated. Excessive or prolonged pressure application can lead to complications such as ischemia-reperfusion injury, nerve damage, and even permanent loss of limb function [1], [2].

A key factor in mitigating these risks is Arterial Occlusion Pressure (AOP)—the minimum pressure required to stop arterial blood flow beyond the tourniquet cuff. Traditionally, AOP is determined through a stepwise increase in cuff pressure while monitoring arterial flow using Doppler ultrasound or pulse oximetry. However, this method is time-consuming and highly operator-dependent, making it impractical for fast-paced surgical and emergency settings [3]. To streamline AOP estimation, several mathematical models have been

<sup>1</sup>Juana Camacho is with the Mechanical Engineering Department and the Biomedical Engineering Department at Universidad de los Andes, Bogota, Colombia. [jvcamacho@uniandes.edu.co](mailto:jvcamacho@uniandes.edu.co)

<sup>2</sup>Jonathan Camargo is with the Mechanical Engineering Department at Universidad de los Andes, Bogota, Colombia. [jon-cama@uniandes.edu.co](mailto:jon-cama@uniandes.edu.co)

proposed, such as Graham's formula, which accounts for systolic and diastolic pressure, limb circumference, and cuff width [1], and Tuncali's model, which incorporates a Tissue Padding Coefficient (KTP) to adjust pressure based on limb compliance [3]. These approaches have contributed to a reduction in tourniquet pressures by 20–40% in adults and more than 50% in children, significantly minimizing pressure-related complications [4].

Despite these advancements, current tourniquet technologies remain limited in their adaptability. They rely on static compression, which does not dynamically adjust to changes in patient physiology, limb movement, or real-time variations in blood pressure. This limitation underscores the need for a more adaptive, patient-specific approach to hemorrhage control.

Soft robotics presents a promising alternative to conventional tourniquets. Unlike traditional rigid systems, soft robotic actuators are made from flexible, deformable materials such as elastomers, allowing for adaptive and compliant interactions with biological tissues [5]. This compliance matching to the human body makes soft robotic devices intrinsically safer and more comfortable for patients. Another key advantage is adaptability: soft actuators can accommodate movement and variations in limb circumference passively, maintaining contact and pressure without requiring complex adjustment mechanisms. Pneumatic networks (PneuNets), originally developed by the Whitesides Research Group, enable controlled inflation of embedded chambers to achieve complex deformations, making them particularly suited for medical applications [6]. In recent years, soft robotic devices have demonstrated success in wearable exoskeletons, rehabilitation gloves, and assistive prosthetics [7]. These technologies offer a compelling opportunity to develop intelligent tourniquets that can self-regulate pressure in response to physiological feedback, reducing the risk of overcompression and ischemic injury.

This study presents the research, design, and fabrication of a soft robotic tourniquet, integrating computational simulations and experimental testing to evaluate its performance. The proposed system leverages soft robotic actuation to apply pressure in a controlled and adaptive manner, optimizing pressure distribution, portability, and safety in both emergency and surgical settings. By bridging the gap between traditional tourniquet technology and soft robotics, this research aims to contribute to the exploration of solutions to achieve the next generation of medical devices, enhancing trauma care, surgical precision, and patient safety.

## II. METHODOLOGY

### A. A Bio-Inspired Tardigrade Model

The proposed design is a bio-inspired model based on the morphology of the tardigrade, a micro-animal known for its resilience and ability to withstand extreme conditions. A key anatomical feature of the tardigrade is its longitudinal dorsal musculature, which extends along the anterior posterior axis and allows contraction of the body [8]. This mechanism is critical for the tardigrade's movement and its principle is reinterpreted in our design as a radial contraction mechanism, implemented by a continuous ring structure with internal chambers. When negative pressure is applied, the structure contracts around the limb, generating an occlusion force suitable for tourniquet applications. To improve retraction and deformation, the chamber size was optimized and connections between modules were eliminated to improve performance. In addition, an internal ring was incorporated to maintain a constant contact area, ensuring a uniformly distributed AOP. Fig. 1 presents an example of the tardigrade anatomy and a conceptual drawing of the proposed geometry.

### B. Simulation

Simulation was used to drive design decisions that defined the shape of the model and operating parameters. The SOFA (Simulation Open Framework Architecture) [9] was used to model and simulate the behavior of the soft robotic structures under different pressure conditions. To perform these simulations, the models were preprocessed as follows:

- 1) **Mesh Preparation:** The STL files of the designs were exported from the design CAD models. These files contained contour and cavity surface geometries.
- 2) **Volume Meshing:** The models were meshed with refined tetrahedrons using Gmsh [10], generating '.msh' files required for the simulation.
- 3) **SOFA Integration:** The 'MeshGmshLoader' component in SOFA was used to import the mesh data, defining the geometry, applying internal negative pressure to the cavity and external forces to observe deformation and device interactions. A hyperelastic material model was used following the parameters from Table I

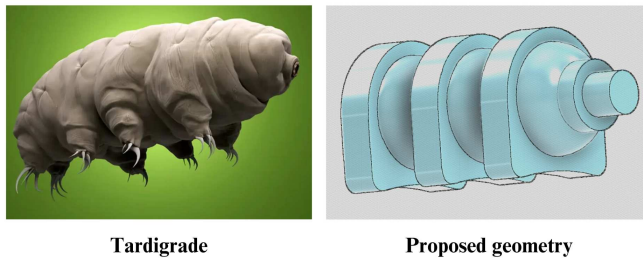


Fig. 1. Tardigrade and sketch of a single module of the tourniquet inspired by the tardigrade anatomy

TABLE I  
PHYSICAL PROPERTIES OF ESQUIM-HC35

Physical Properties	ESQUIM-HC35
Hardness (Shore A)	35
Mixing Ratio (by weight)	100A:100B
Color	Skin color / Transparent
Viscosity (cps)	6000 - 8000
Working Time	20 - 30 mins
Curing Time	10 - 12 hours
Tear Strength (KN/m)	$\geq 13$
Tear Strength (MPa)	$\geq 2.2$
Elongation (%)	$\geq 380\%$

The simulation was conducted in a zero-gravity environment ('root.gravity = [0, 0, 0]') to isolate the effects of internal actuation. A surface pressure of -10000 Pa was applied to the internal cavity ('SurfacePressureForceField'), with a pressure variation speed of 15000 Pa/s to simulate actuation. The mechanical response was computed using an implicit time integration scheme, employing an Euler implicit solver ('EulerImplicitSolver') and a conjugate gradient linear solver ('CGLinearSolver'), configured with 100 iterations and a tolerance of  $10^{-5}$ .

To account for interactions with external rigid bodies, the simulation incorporated collision detection mechanisms, including 'BruteForceDetection', 'MinProximityIntersection', and 'PointCollisionModel', ensuring that the soft structure's deformation remained physically consistent.

### C. Materials and Fabrication Process

The elastomer ESQUIM-HC35 was selected based on its mechanical properties, biocompatibility, and suitability for soft robotics applications [11]. The materials were degassed using a vacuum chamber to remove air bubbles prior to curing. The curing process followed the manufacturer's recommendations shown in Table I including the use of mold release silicone spray [11].

To create the tourniquet geometry, a single silicone casting process was designed using two molds and a core (Fig. 2). The two molds were aligned with screws, which also reduce the silicone flash. The core of this model was 3D printed using polyvinyl alcohol (PVA) filament with the objective of dissolving this structure in water to create the ring cavity once the silicone was cured. The core is then inserted into cylinders with low tolerance, which keep the core aligned in the center of the ring. The assembled mold is shown in Fig. 3.

### D. Controller Architecture

An actuation system was designed around the ESP32-WROOM microcontroller, chosen for its low power consumption and high efficiency. The system architecture is divided into two functional blocks:

- **Air-Pump Control:** A relay module with optocoupler relays was used to switch the MAC valves connected to the air and vacuum pumps. A SPDT switch allowed

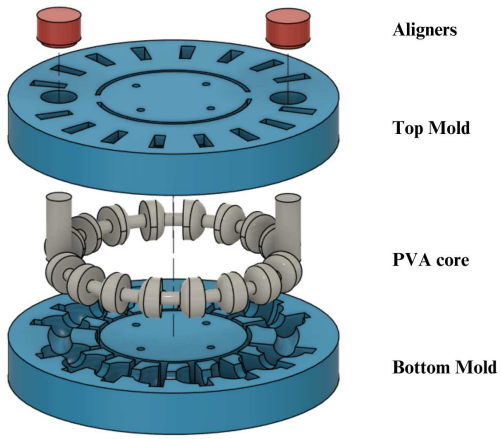


Fig. 2. Exploded view of the casting mold system. The mold consists of two exterior parts, a PVA core, and aligners.

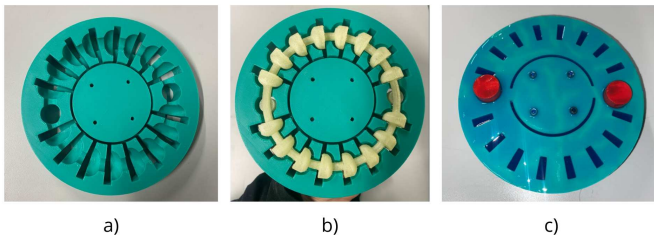


Fig. 3. a) Upper mold, b) Upper mold with the core inserted, c) Assembled mold filled with ESQUIM-HC35

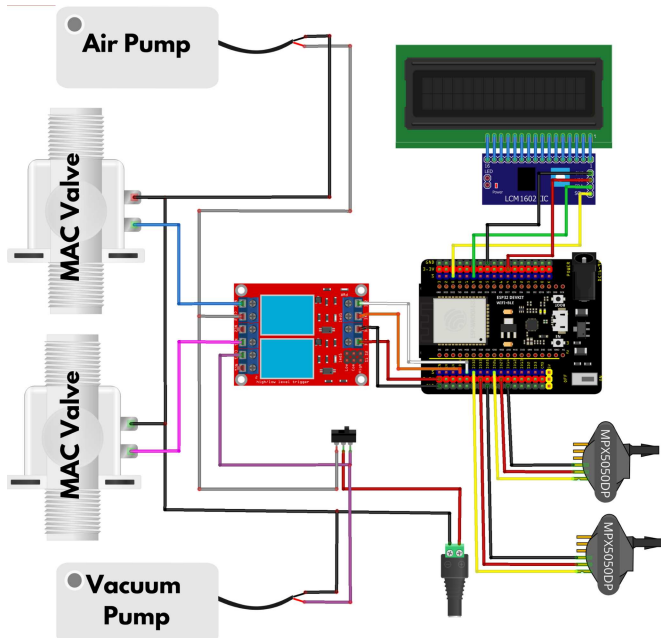


Fig. 4. Electronic circuit implemented in the portable device. ESP32-based controller circuit schematic integrating dual-mode air/vacuum pump control with relay modules, MPX5050DP sensor pressure monitoring, and I2C LED display linked to a PC for mode and target pressure settings.

for toggling between positive and negative pressure operation.

- **Pressure Logging and Visualization:** Two MPX5050DP pressure sensors were integrated for real-time monitoring. An LED display with an I2C adapter was used to visualize the pressure exerted by each pump.

The implemented controller shown in Fig. 4, operates while establishing a serial communication link between the Main Controller Unit (ESP32) and a PC, where the pump operating mode is set, vacuum or air.

Next, the target pressure is defined. Once initialized, an on-off control mechanism is applied, using the pressure reported by the MPX5050DP transducers as the reference value. These transducers send an analog signal to the ADC pins of the microcontroller, and by applying the linear regression equation provided in the manufacturer's datasheet, a pressure value in kPa is obtained and displayed on the LCD screen.

Subsequently, a signal is sent to activate or deactivate the relay corresponding to the MAC-type valve, depending on whether it is for vacuum or air. This allows the airflow to circulate through each of the pneumatic hoses accordingly.

This device has both, vacuum pump and air pump because it was created for testing other proposed designs of soft-tourniquets, some of which were designed to work with positive pressure.

To integrate the pneumatic and electronic components into a compact form factor, a custom enclosure was designed and 3D-printed. The assembled device, including all components, is presented in Fig. 5.

#### E. Experimental validation

Preliminary tests were done during the iterative process of prototyping and geometry refinement. These tests involved using a vacuum pump and manometer while observe the contraction and vacuum pressure of the resulting tourniquets.

For the final iteration we used an *Advanced Venipuncture Arm* from *Limbs & Things* [12] in the Medical Skills and Simulation laboratory of the Faculty of Medicine at the Universidad de los Andes, located at the *Fundación Santa Fe de Bogotá*. This model is anatomically correct and can be used to accurately simulate venipuncture, intravenous cannulation, and intravenous infusion. The venipuncture arm was used to evaluate the ease of placement on the limb and the interaction with the arm as shown in Fig. 6.

### III. RESULTS

Simulations were used to drive the development process for the shape and cavities for the model. We analyzed the behavior of the modules under negative pressure and their effect on the variation of the ring's diameter. The main simulation results are presented in Fig. 8 with the meshed volume shown in Fig. 7. It consists of six modules forming a ring.

The deformation profile patterns confirmed the expected contraction behavior when adapting the proposed module geometry into a ring. This behavior was validated in an initial

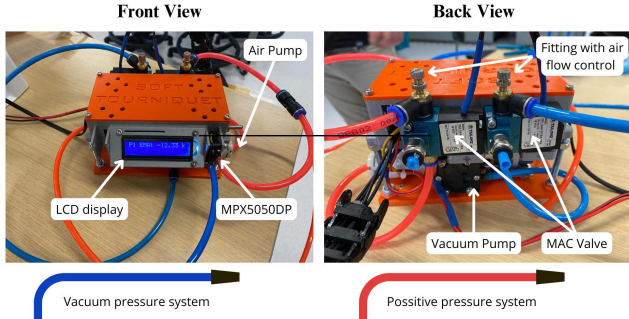


Fig. 5. Assembled device for experimental validation. The system includes the electronic circuit and the pneumatic circuit assembled in a 3D-printed enclosure.

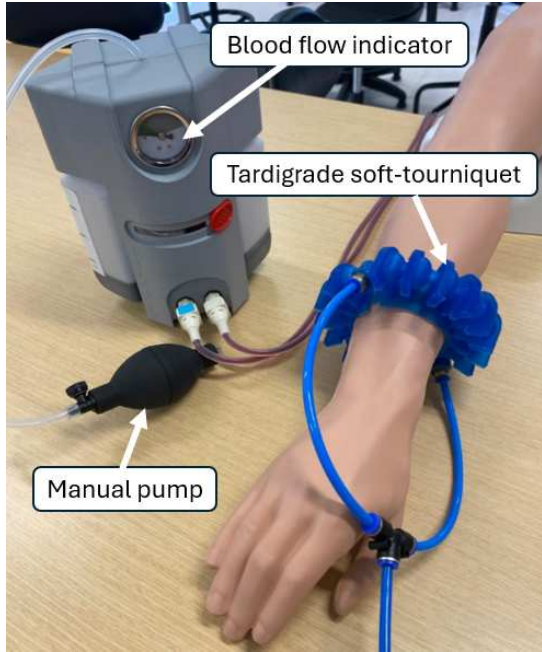


Fig. 6. Tourniquet tested in an Advanced Venipuncture Arm in the Medical Skills and Simulation laboratory of Universidad de los Andes.

version of the ring, shown in Fig. 9. Subsequently, an internal ring was added to the design to improve the radial contraction force exerted by the tourniquet and to provide a uniform contact area. The final design is presented in Fig. 11. Furthermore, a tardigrade-inspired module demonstrated successful contraction and deformation when tested using a syringe, as shown in Fig. 10, achieving a contraction of 60.98%.

However, when constructing the complete ring, we observed an issue where the tubes connecting the modules collapsed under negative pressure. This collapse obstructed airflow through the cavities, which in turn affected the contraction of sections that were farther from the air outlet. Through the iterative process involving simulation and prototyping, we finally achieved the model presented in Fig. 11 with an increased chamber size of 61.95%, and having a final volume of 38.0mL in the relaxed state.

The deformation of this model was tested in isolation (Fig. 12) and when placed on the venipuncture arm (Fig. 13). We

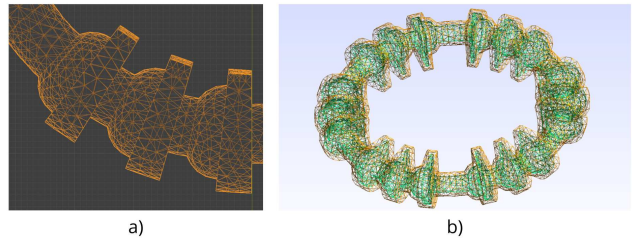


Fig. 7. a) Tourniquet exterior mesh, b) Meshed volume in Gmsh generated by the surface and the cavity meshes. This meshed model was used to analyze the deformation behavior under different pressure conditions.

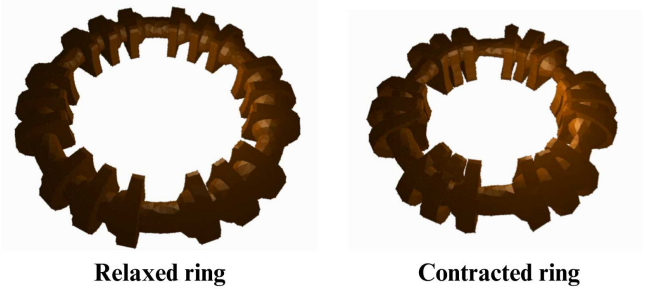


Fig. 8. Simulation results in SOFA for the soft tourniquet ring in relaxed and contracted state.

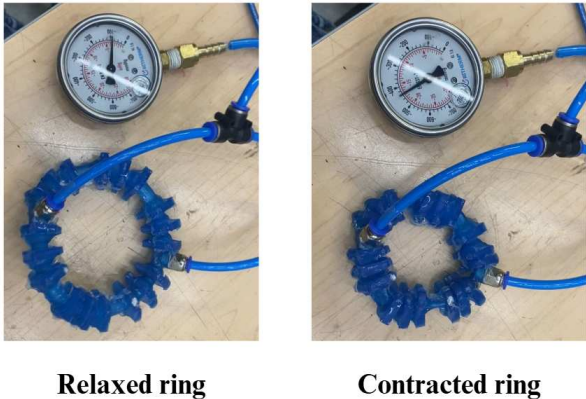
observed that the tourniquet achieved a consistent contraction with a decrease of 53.95% in the diameter.

#### IV. DISCUSSION

The iterative design and fabrication process demonstrated that combining simulation and physical prototyping could successfully yield a functional soft robotic tourniquet with dynamic pressure adjustment capabilities. The use of two-part PLA molds and a PVA core was an effective manufacturing strategy for producing the complex geometries required for this design. Additionally, mold release spray played a crucial role in ensuring ease of part demolding without damaging the delicate soft structures.

Simulations were instrumental in understanding the behavior of the modules under negative pressure and provided valuable insights into the contraction dynamics, although they are not without limitations and should be considered as one tool in informing the design process. The results of the simulations, when validated experimentally, confirmed the qualitative deformation and retraction of the modules. This feedback loop of simulation and testing enabled us to refine the design with respect to the contraction mechanism.

However, during early prototype testing, we encountered challenges related to the tube collapse under negative pressure, which hindered airflow between the modules. This problem was rectified by eliminating the connecting tubes and increasing the chamber size, which ultimately improved the contraction and ensured consistent retraction during experimental validation. The resulting model demonstrated a significant 53.95% reduction in diameter, which aligns closely with the predictions made in our simulations.



Relaxed ring

Contracted ring

Fig. 9. First version of the soft tourniquet ring in relaxed and contracted state.

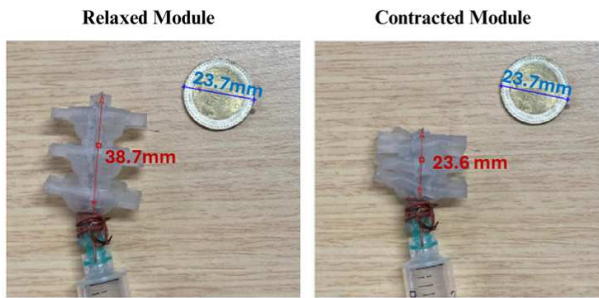


Fig. 10. Deformation of a single module under pressure variation. The figure shows the module in its relaxed (left) and contracted (right) states. Negative pressure causes the module to shrink, demonstrating its deformation capability. A reference coin is included for scale

One of the key challenges identified in this study was the uneven contraction of the tourniquet in its final state. The internal ring, originally intended to maintain uniform arterial occlusion pressure (AOP) around the limb, caused the tourniquet to deform asymmetrically, leading to an eye-shaped contraction pattern. This limitation suggests that further refinement of the internal geometry may be necessary to achieve more consistent pressure distribution. Despite this, the increased chamber size and removal of inter-module connections proved effective in achieving better contraction.

While the current prototype relies on pre-defined target pressures set via external control, a critical future development will be the integration of real-time arterial pressure sensing and feedback control. This would allow the tourniquet to dynamically adjust its pressure based on continuous physiological feedback, ensuring that the applied pressure is sufficient to achieve occlusion without exceeding safe thresholds. Potential approaches include doppler ultrasound sensors to detect the cessation of arterial flow directly or embedding pressure sensors along the internal surface of the tourniquet to monitor contact pressure distribution and adjust negative pressure accordingly.

Another key limitation of this study is the lack of testing on human subjects or anatomically realistic soft tissue models. The venipuncture arm provided a useful preliminary

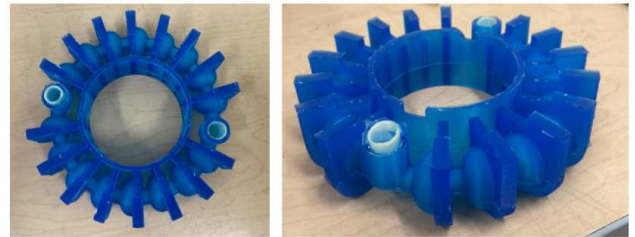


Fig. 11. Manufactured tardigrade-inspired soft tourniquet. The left image shows a top-down view of the structure, highlighting its circular arrangement and evenly distributed actuation chambers. The right image provides an angled perspective, showcasing the integration of inlet ports for pneumatic actuation.

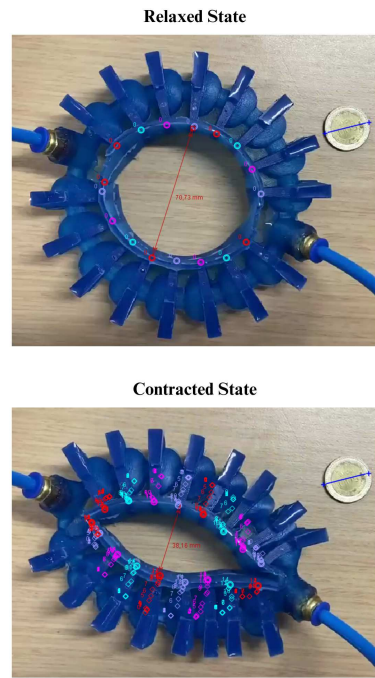


Fig. 12. Deformation of the tourniquet under contraction. The figure shows the tourniquet in its relaxed (top) and contracted (bottom) states. Negative pressure causes the actuation chambers to collapse, reducing the internal diameter and exerting constriction. Tracker generated the movement trace along the walls, providing a visual representation of deformation. A reference coin is included for scale.

evaluation platform, but future work should include cadaver studies or high-fidelity limb phantoms capable of simulating both vascular response and tissue compliance under dynamic loading. This would allow a more direct assessment of the device's ability to achieve AOP without excessive tissue compression, further validating the safety and efficacy of the soft robotic tourniquet.

## V. CONCLUSION

The tardigrade-inspired soft-robotic tourniquet developed in this study demonstrates significant potential for dynamic pressure regulation in emergency medical applications. By enabling the dynamic adjustment of pressure to achieve the device can potentially reduce the risk of excessive tissue

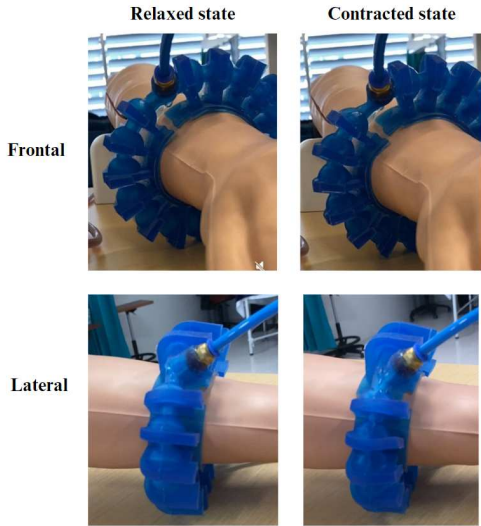


Fig. 13. Tourniquet tested on the venipuncture arm in relaxed and contracted states. The figure shows the soft robotic tourniquet applied to a venipuncture training arm. The frontal and lateral views illustrate its deformation when transitioning from the relaxed (left) to the contracted (right) state due to applied negative pressure. This test evaluates the device's ability to conform to the limb and apply uniform constriction.

damage, apoptosis, and thrombosis typically associated with traditional static pressure tourniquets. The combination of simulation-driven design and iterative prototyping resulted in a device capable of considerable deformation and contraction, making it a promising candidate for further development in soft robotics for medical applications.

The achieved significant contraction in the final model aligning with the desired pressure characteristics, demonstrating the effectiveness of the design. However, to move forward, it is essential to address the issue of uneven contraction and improve the internal geometry to ensure uniform AOP around the limb. Furthermore, testing with a more accurate anatomical model would help validate the efficacy of the design in real-world conditions.

Future work should explore advanced materials that can better mimic human tissue compliance, integration with real-time pressure sensors to monitor AOP, and further refinement of the design for ease of use in clinical settings. Additionally, real-world clinical trials will be essential to determine the device's performance in actual emergency medical situations, which could ultimately lead to improved outcomes for patients suffering from hemorrhagic events.

## REFERENCES

- [1] J.-P. Estebe, J. M. Davies, and P. Richebe, “The pneumatic tourniquet: Mechanical, ischaemia–reperfusion and systemic effects,” *European Journal of Anaesthesiology*, vol. 28, no. 6, pp. 404–411, 2011. DOI: 10.1097/EJA.0b013e328346d5a9.
- [2] L.-A. Van der Spuy, “Complications of the arterial tourniquet,” *South African Journal of Anaesthesia and Analgesia*, vol. 18, no. 1, pp. 14–18, 2012. DOI: 10.1080/22201173.2012.10872769.
- [3] B. Tuncali, A. Karcı, B. Erdalkiran Tuncali, *et al.*, “A new method for estimating arterial occlusion pressure in optimizing pneumatic tourniquet inflation pressure,” *Anesthesia & Analgesia*, vol. 102, no. 6, pp. 1752–1757, 2006. DOI: 10.1213/01.ane.0000209018.00998.24.
- [4] P. G. Fitzgibbons, C. DiGiovanni, S. Hares, and E. Akelman, “Safe tourniquet use: A review of the evidence,” *Journal of the American Academy of Orthopaedic Surgeons*, vol. 20, no. 5, pp. 310–319, 2012. DOI: 10.5435/JAAOS-20-05-310.
- [5] L. Garcia, G. Kerns, K. O'Reilly, *et al.*, “The role of soft robotic micromachines in the future of medical devices and personalized medicine,” *Micromachines*, vol. 13, no. 1, p. 28, Dec. 2021, ISSN: 2072-666X. DOI: 10.3390/mi13010028. [Online]. Available: <http://dx.doi.org/10.3390/mi13010028>.
- [6] A. C. Panagiotis Polygerinos Bobak Mosadegh, *Pneunets bending actuators*, Accessed: 2024-06-20, 2024. [Online]. Available: <https://softroboticstoolkit.com/book/pneunets-bending-actuator>.
- [7] D. Rus and M. T. Tolley, “Design, fabrication and control of soft robots,” *Nature*, vol. 521, pp. 467–475, 2015. DOI: 10.1038/nature14543.
- [8] D. K. Persson, K. A. Halberg, R. C. Neves, A. Jørgensen, R. M. Kristensen, and N. Møbjerg, “Comparative myoanatomy of tardigrada: New insights from the heterotardigrades actinarctus doryphorus (tanarctidae) and echiniscoides sigismundi (echiniscoididae),” *BMC Evolutionary Biology*, vol. 19, no. 1, Nov. 2019, ISSN: 1471-2148. DOI: 10.1186/s12862-019-1527-8. [Online]. Available: <http://dx.doi.org/10.1186/s12862-019-1527-8>.
- [9] F. Faure, C. Duriez, H. Delingette, *et al.*, “SOFA: A Multi-Model Framework for Interactive Physical Simulation,” in *Soft Tissue Biomechanical Modeling for Computer Assisted Surgery*, ser. Studies in Mechanobiology, Tissue Engineering and Biomaterials, Y. Payan, Ed., vol. 11, Springer, Jun. 2012, pp. 283–321. DOI: 10.1007/8415\\_2012\\_125. [Online]. Available: <https://inria.hal.science/hal-00681539>.
- [10] Geuzaine, Christophe and Remacle, Jean-François, *Gmsh*, version 4.6.0, Jun. 22, 2020. [Online]. Available: <http://gmsh.info/>.
- [11] E. D. C. C. LTDA, *Esquim hc-35: Silicona de platino-curado para la industria de la salud*, Available online: <https://www.esquim.com/elastomeros-rtv/> (Accessed: 2024-07-29), 2024.
- [12] Limbs Things, *Advanced venipuncture arm – light skin tone*, Accessed: 2025-03-02, 2025. [Online]. Available: <https://limbsandthings.com/us/products/70300-advanced-venipuncture-arm-light-skin-tone/>.